Effects of local gas-flow field on synthesis of oxide nanowires during thermal oxidation

ChunHua Xu,[1] XiangLong Yang,[2] San-Qiang Shi,[2,a)] Yang Liu,[2] Charles Surya,[1] and ChungHo Woo[1]
[1]*Department of Electronic Information Engineering, The Hong Kong Polytechnic University, Hunghom, Kowloon, Hong Kong, China*
[2]*Department of Mechanical Engineering, The Hong Kong Polytechnic University, Hunghom, Kowloon, Hong Kong, China*

(Received 16 April 2008; accepted 15 May 2008; published online 27 June 2008)

Ω-shaped copper specimens are oxidized in wet air. The results show that totally no-wire structure, CuO whiskers, and the high density of well-aligned CuO nanowires can be formed simultaneously on the different positions of the specimen. A three-dimensional flow simulation results indicate that the direction of velocity vectors of local gas flow affects the alignment of nanowires during oxidation while the shear stress of flowing gas near the surface of a Ω-shaped specimen controls the density of nanowires. © *2008 American Institute of Physics*. [DOI: 10.1063/1.2940597]

One-dimensional nanostructure materials[1] have become an important research field in both science and technology. One-dimensional nanostructure provides a platform to investigate the relationship between the properties of materials with dimensionality and size.[2–6] They are also expected to play important roles for nanodevices and integrated nanosystems.[7,8] Up until now, one-dimensional nanostructures, including nanowire, nanobelt, and nanotube, have been produced using various synthetic approaches, such as vapor-phase evaporation,[9] chemical vapor deposition,[10] sol gel,[11] template-based method,[12] arc discharge,[13] laser ablation,[14] and solution.[15] A simple method of synthesis of oxide nanowires by thermal oxidation of metals has been reported recently.[16–18]

In fact, oxide whiskers growing on the surface of metals during thermal oxidation was observed nearly half a century ago.[19] Compared to whiskers, nanowires are characterized to have a long length, a small diameter, or very high density. The precise conditions under which the growth of whiskers/nanowires by thermal oxidation occurs remain unclear. Cold work of metals has been found to favor whisker growth.[20] The oxidative environment, such as oxygen pressure,[21] composition of gas,[17,20,21] oxidation temperature, and time[16,21] can greatly affect the formation of nanowires. Favorable growth of nanowires is on specimens with small size.[22] We report that totally no-wire structure, CuO whiskers, and the high density of well-aligned CuO nanowires can be formed simultaneously on the different positions of the specimen during thermal oxidation in this paper.

Commercial Cu foils with thickness of 0.1 mm (purity: 99.9% Cu) are cut to the size of about 38×4 mm^2, which is made into Ω-shaped specimens [see Fig. 1(a)]. Specimens are then washed in an aqueous solution of 1.5*M* HCl for 1 min, rinsed in de-ionized water, and then dried in nitrogen, before oxidized in a Lindberg tube furnace with diameter of 52 mm and length of 850 mm. The specimens are placed in an alumna crucible at 500 °C for 4 h in flowing wet compressed air[21] at a pressure of 1 atm and an inlet gas-flow rate of 1.0 l/min. The flow-rate of inlet gas is measured by a Platon gas-flow meter. Morphologies of the oxidized specimens are characterized with a scanning electron microscope (STEREOSCAN 440). To prepare samples for transmission electron microscopy (TEM) examination, a bottle of the ethanol solution with the oxide scales is placed in an ultrasonic machine (COLE-Parmer 8890) for 10 min. Then, the resulting solution is dropped onto a carbon coated TEM grid. TEM image is performed on the samples on the TEM grid using a JEOL 2010F TEM, operated at 200 kV.

A coordinate system in Fig. 1(b) is defined to describe the positions on the surface of a Ω-shaped specimen. Where the angle θ changes from 0 to 360° in anticlockwise direction and subscripts *in* and *out* are responsible for the inner and outer surfaces of Ω-shaped specimens, respectively. For example, $\angle 90_{in}$ means the position of $\theta=90°$ and the inner surface of a Ω-shaped specimen, as illustrated in Fig. 1(b).

Almost no-wire structure can be found on the positions of $\angle 120_{out}$-$\angle 230_{out}$ and $\angle 280_{out}$-$\angle 320_{out}$. As an example, Fig. 2(a) illustrates complete absence of nanowires at the position of $\angle 180_{out}$. The low density of nanowires are formed on the other positions of the outer surfaces of a

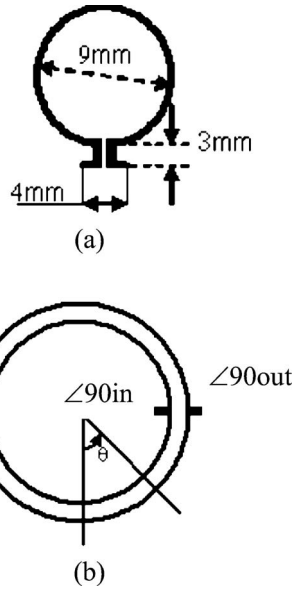

FIG. 1. (a) The front view of the dimensions of a Ω-shaped specimen (b) coordinate system to define the positions on the surfaces of a Ω-shaped specimen.

a)Author to whom correspondence should be addressed. Electronic mail: mmsqshi@polyu.edu.hk.

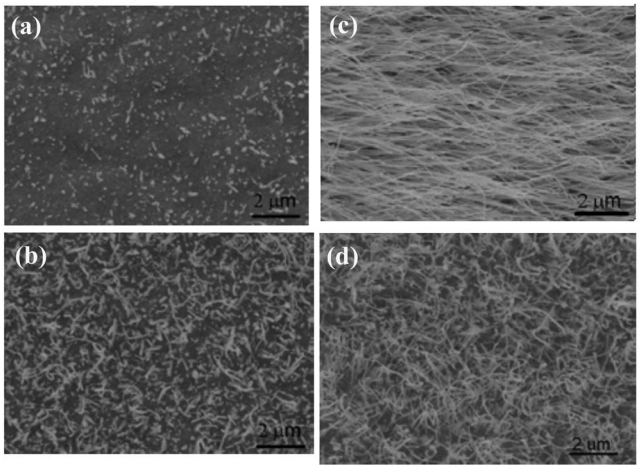

FIG. 2. Typical morphologies of nanowires formed on Ω-shaped specimens after the oxidation in wet air at an inlet gas-flow rate of 1.0 l/min; scanning electron microscopy images show (a) nearly no-wire structure on the position of $\angle 180_{out}$; (b) the low density of random orientation of nanowires on the position of $\angle 45_{out}$, (c) the extremely high density of the well-aligned nanowires on the positions of $\angle 185_{in}$, and (d) the high density of random orientation nanowires on the position of $\angle 90_{in}$.

Ω-shaped specimen. Figure 2(b) shows a low density of random distribution of nanowires at the position of $\angle 45_{out}$. In general, the density of nanowires on the outer surface of the specimens is lower than that on the inner surface. The density of nanowires in the position of $\angle 180_{in}$-195_{in} is the highest. Interestingly, the nanowires in this range are well aligned. Figure 2(c) shows the morphologies of nanowires at the position of $\angle 185_{in}$ of the Ω-shaped specimen. The nanowires at the other positions of the inner surface of the specimens are not well aligned but with high density. Figure 2(d) shows the morphology of the nanowires at the position of $\angle 90_{in}$.

TEM image of a typical nanowire with diameter of about 50 nm is shown in Fig. 3. The inset on top right is the corresponding selected area electron diffraction pattern of the nanowire, revealing the monoclinic structure of CuO. A high resolution image taken on this nanowire inserted at the left bottom in Fig. 3 shows a lattice space of 1.71*A* (0 2 0) plane of monoclinic CuO. The crystal structure of oxide nanowires formed on copper during oxidation is monoclinic CuO from

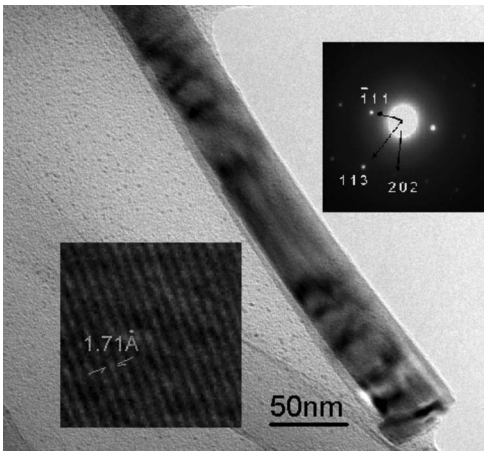

FIG. 3. TEM image of a typical CuO nanowire with diameter of about 50 nm. The inset on top right is the corresponding selected area electron diffraction pattern of the nanowire, revealing the monoclinic structure of CuO. The inset on left-bottom is the HRTEM of the nanowire, showing a lattice space of 1.71 Å on (020) plane of monoclinic CuO.

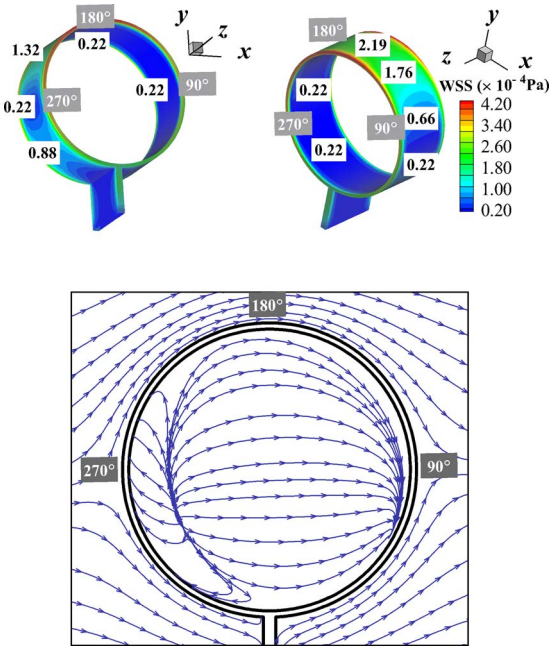

FIG. 4. (Color online) Computer simulation of local gas-flow field around the specimen: (a) the distribution of the wall shear stresses around the specimen from the left and right views and the values are local wall shear stresses; (b) the flow pathlines of gas on the middle cross section of specimen.

our and other researchers' reports,[16,21] which is the same as whiskers formed on copper.[23] The nanowire consisting of higher valence oxide is explained based on the oxidation thermodynamics.[22]

In order to understand thoroughly the observed phenomenon and investigate the effect of the gas-flow field on the growth of nanowires, a three-dimensional flow simulation is carried out using a Computational Fluid Dynamics solver (Fluent). The computational model and boundary conditions are the same as those in the experiment, and the inlet gas-flow rate is selected as 1.0 l/min. The wall shear stress (the shear stress of flowing gas near the surface of the specimen) τ is expressed as

$$\tau = \mu \frac{\partial \vec{v}}{\partial \vec{n}}, \tag{1}$$

where μ is the dynamic viscosity of the gas, $\partial \vec{v}/\partial \vec{n}$ is the velocity gradient of the gas flow, $\vec{v}$ is velocity, and $\vec{n}$ is the normal vector of the wall surface. Figure 4(a) shows the distribution of wall shear stress around a Ω-shaped specimen from the left- and right-side views. The values in Fig. 4(a) are wall shear stress on the positions of the related surface. Comparing Fig. 2 to Fig. 4(a), it can be concluded that the density of nanowires relates strongly to the local wall shear stresses. Nanowires can be formed on the positions where the wall shear stress is less than 2.5×10^{-5} Pa, as shown in dark blue color in Fig. 4(a), in which nanowires in forms as illustrated in Fig. 2(b) at position $\angle 45_{out}$, Fig. 2(c) at $\angle 185_{in}$, and Fig. 2(d) at $\angle 90_{in}$ can be observed. However, almost no-wire structure can be found at positions $\angle 120_{out}$-$\angle 240_{out}$ and $\angle 280_{out}$-$\angle 320_{out}$ [see Fig. 2(a)], where the local wall shear stress is over 2.5×10^{-5} Pa. The flow pathlines around the middle cross section of specimen are shown in Fig. 4(b) (front view). The direction of the flow path lines of flowing gas are shown by the arrowed lines and are generally from left to right. The typical morphology on the surface of

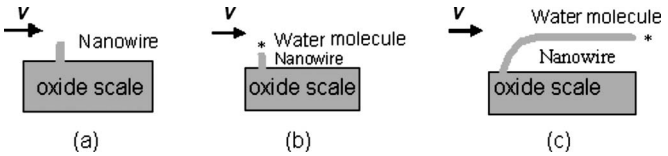

FIG. 5. Schematic illustration of the effects of the velocity vectors (v) of flow gas on the growth of nanowires: (a) initial oxidation; (b) water molecule adsorbed on the top tip of a nanowire, and (c) nanowire growth along the direction of velocity vectors of flow gas.

the oxidized Ω-shaped specimen at the positions of $\angle 180_{in}$-$\angle 195_{in}$ in Fig. 2(c) shows the high density of well-aligned nanowires. The magnitude of the wall shear stresses at this range is less than 2.5×10^{-5} Pa. Moreover, the alignment direction of nanowires coincides with the direction of main gas flowing at inner specimen (from left to right). The results indicate that the direction of the growth of nanowires may relate to the direction of the velocity vectors of the flow gas.

Ω-shaped specimens are also oxidized in dry air (compressed air is directly used as the oxidative gas). The density of oxide nanowires on the whole specimen after oxidation in dry air is much lower than that after oxidation in wet air. It has been reported that water vapor in oxidative gas can enhance the formation of whiskers[20] and nanowires[21] during thermal oxidation. The physical mechanism of water vapor on whisker growth has not been understood so far. The presence of water vapor seems to affect the high temperature creep of the oxide scale. Therefore, water vapor perhaps has more far-reaching effects.[24]

From the analysis above, nanowires can be formed at the positions of the wall shear stress of less than 2.5×10^{-5} Pa in wet air. Nanowires in Fig. 2(c) are shown to align along the direction of the main gas flow [see Fig. 4(b)]. The mechanism of the nanowire growth, including the density and alignment, is schematically illustrated in Fig. 5. Water vapor can be easily adsorbed on the surface of oxide scale where there is low wall shear stress. Since the gas velocity on the surface of specimen is zero, lower velocity near the wall indicates lower velocity gradient, i.e., lower wall shear stress. Based on the theory of fluid mechanics, a high pressure can be produced on the solid surface where there is low gas velocity (or low wall shear stress).[25] According to the theory of the adsorption of gas, the higher the pressure, the more the adsorbed molecules on solid surface.[26] In other words, more water molecules can be adsorbed on the location of scale where there is low wall shear stress. Water vapor can be easily adsorbed on the defects, such as dislocations, of the oxide scale at the positions of low wall shear stress, such as the position of $\angle 180_{in}$, during initial oxidation. A nucleus of nanowire can be formed on the area with more water molecules in Fig. 5(a). Then, water vapor may be adsorbed on the tip of a nanowire in Fig. 5(b) and the nanowire will continue to grow along the direction of velocity vectors of the flow gas, as indicated in Fig. 5(c).

When the wall shear stress τ is high, such as the position of $\angle 180_{out}$, low pressure at that area can reduce the adsorbed water molecules therefore, resulting in the low density of nanowires. If the oxidation process of a Ω-shaped specimen occurs in dry air, the formation of nanowires becomes difficult even at the positions where there is low wall shear stress due to less adsorbed water molecules.

In summary, we have demonstrated that the local gas-flow field around Ω shaped specimens can significantly affect the morphologies of CuO oxide nanowires formed during thermal oxidation of copper. Totally no-wire structure, whiskers, and the high density of well-aligned nanowires can be formed simultaneously at various positions of Ω-shaped specimens after the oxidation in flowing wet air. The velocity vectors of local flow gas affect the growth direction of nanowires during oxidation while the wall shear stress controls the density of nanowires. Nanowires can easily form at positions, where the wall shear stress is less than 2.5×10^{-5} Pa. The extremely high density of the well-aligned CuO nanowires with diameters between 30 and 80 nm and length of 10 μm can be grown on the top position of the inner side of a Ω-shaped specimen. The density of oxide nanowires will be significantly reduced, when a Ω-shaped specimen is oxidized in dry air.

This work was funded by research Grants from PolyU G-U344, G-YF66, PolyU5312/03E, PolyU5309/03E, and PolyU 5236/04E.

[1] Z. W. Pan, Z. R. Dai, and Z. L. Wang, Science **291**, 1947 (2001).
[2] D. S. Hopkins, D. Pekker, P. M. Goldbart, and A. Bezryadin, Science **308**, 1762 (2005).
[3] J. D. Holmes, K. P. Johnston, R. C. Doty, and B. A. Korgel, Science **287**, 1471 (2000).
[4] L. D. Hicks and M. S. Dresselhaus, Phys. Rev. B **47**, 16631 (1993).
[5] M. H. Hung, S. Mao, H. Feick, H. Yan, Y. Wu, H. Kind, E. Weber, R. Russo, and P. Yang, Science **292**, 1897 (2001).
[6] E. W. Wong, P. E. Sheehan, and C. M. Lieber, Science **277**, 1971 (1997).
[7] X. F. Duan, Y. Huang, R. Agarwal, and C. M. Lieber, Nature (London) **421**, 241 (2003).
[8] A. Kolmakov, D. O. Klenov, Y. Lilach, S. Stemmer, and M. Moskovits, Nano Lett. **5**, 667 (2005).
[9] Z. L. Wang, Z. W. Pan, and Z. R. Dai, U.S. Patent No. 6,586,095 (July 1, 2003).
[10] M. Yazawa, M. Koguchi, A. Muto, M. Ozawa, and K. Hiruma, Appl. Phys. Lett. **61**, 2051 (1992).
[11] M. Adachi and T. Harada, Langmuir **15**, 7097 (1999).
[12] E. Braun, Y. Eichen, U. Sivan, and G. Ben-Yoseph, Nature (London) **391**, 775 (1998).
[13] Y. C. Choi, W. S. Kim, Y. S. Park, S. M. Lee, D. J. Bae, H. Y. Lee, G. S. Park, W. B. Choi, N. S. Lee, and J. M. Kim, Adv. Mater. (Weinheim, Ger.) **12**, 746 (2000).
[14] A. M. Morales and C. M. Leiber, Science **279**, 208 (1998).
[15] T. J. Trentler, K. M. Hickman, S. C. Goel, A. M. Viano, P. C. Gibbons, and W. E. Buhro, Science **270**, 1791 (1995).
[16] X. Jiang, T. Herricks, and Y. Xia, Nano Lett. **2**, 1333 (2002).
[17] Y. Y. Fu, R. M. Wang, J. Xu, J. Chen, Y. Yan, A. V. Narlikar, and H. Zhang, Chem. Phys. Lett. **379**, 373 (2003).
[18] G. Gu, B. Zheng, W. Q. Han, S. Roth, and J. Liu, Nano Lett. **2**, 849 (2002).
[19] R. Takagi, J. Phys. Soc. Jpn. **12**, 1212 (1957).
[20] G. M. Raynaud and R. A. Rapp, Oxid. Met. **21**, 89 (1984).
[21] C. H. Xu, C. H. Woo, and S. Q. Shi, Superlattices Microstruct. **36**, 31 (2004).
[22] C. H. Xu, C. H. Woo, and S. Q. Shi, Chem. Phys. Lett. **399**, 62 (2004).
[23] P. Kofstad, *High Temperature Oxidation of Metals* (Wiley, New York, 1967).
[24] P. Kofstad, *High Temperature Corrosion* (Elsevier Applied Science, London and New York, 1988).
[25] J. F. Douglas, J. M. Gasiorek, and J. A. Swaffield, *Fluid Mechanics*, 3rd ed. (Longman Scientific and Technical, New York, 1995).
[26] L. I. Osipow, *Surface Chemistry: Theory and Industrial Application* (Reinhold, New York, 1962).